

**Supplementary Information:**

**Selective Deposition of Pt onto Supported Metal Clusters for Fuel Cell  
Electrocatalysts**

Tae-Yeol Jeon,<sup>a</sup> Nicola Pinna,<sup>a,b</sup> Sung Jong Yoo,<sup>c</sup> Docheon Ahn,<sup>d</sup> Sun Hee Choi,<sup>d</sup> Marc-Georg Willinger,<sup>e</sup> Yong-Hun Cho,<sup>f</sup> Kug-Seung Lee,<sup>c</sup> Hee-Young Park,<sup>a</sup> Seung-Ho Yu,<sup>a</sup> and Yung-Eun Sung \*<sup>a</sup>

**Contents:**

- 1. Atomic ratio of Pt to Pd of Pt[0.5]/Pd/C obtained from energy-dispersive X-ray spectroscopy (EDS)**
- 2. TEM images of as-prepared Ru/C and Pd/C**
- 3. TEM images and particle size distribution histograms of Pd/C, Pt[0.1]/Pd/C, Pt[0.3]/Pd/C, and Pt[0.5]/Pd/C**
- 4. ORR currents of Pt[0.2-1.4]/Ru/C and Pt[0.1-0.7]/Pd/C**
- 5. Refined lattice parameters of Ru-Pt core-shell nanoparticles from powder X-ray diffraction**
- 6. Detailed EXAFS parameters of Pd- and Ru-Pt core-shell nanoparticles**

## 1. Atomic ratio of Pt to Pd of Pt[0.5]/Pd/C obtained from energy-dispersive X-ray spectroscopy (EDS)

Although chemical composition of all samples was obtained from ICP-AES, EDS was also carried out for more credibility. Pt[0.5]/Pd/C, which had the highest mass(Pt)-specific ORR activity, showed a slightly higher ratio of Pt to Pd, as compared to the ICP-AES result (Pt:Pd = 34.1:65.9).

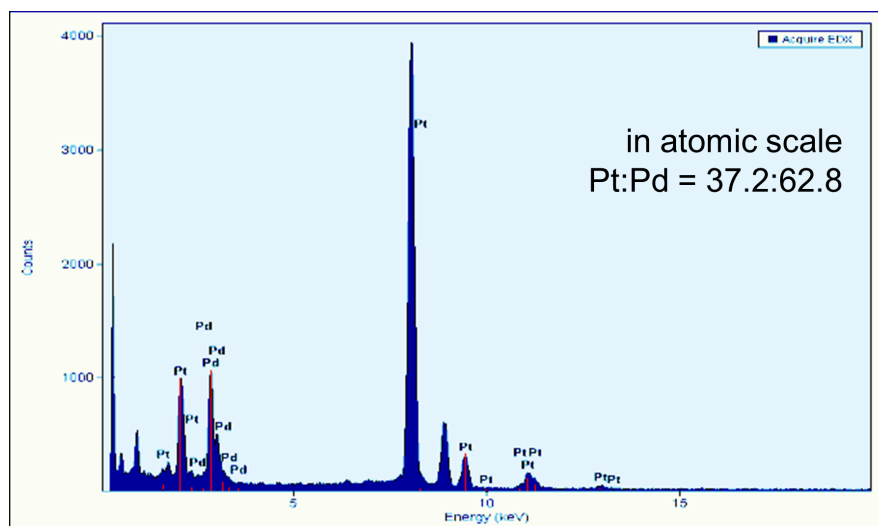


**Figure S1.** EDS analysis on Pt[0.5]/Pd/C.

## 2. TEM images of as-prepared Ru/C and Pd/C

Size distribution, particle shape, and distribution were confirmed by transmission electron microscopy (TEM, FEI Tecnai F20 and JEOL 2010 at 200 kV). Figure S2a and b shows as-prepared Ru/C (21.1 wt %) and Pd/C (28.4 wt %), respectively. As-prepared Ru nanoparticles have an average particle size of ca. 1.6 nm. To increase the particle size and the crystallinity of Ru, heat-treatment was carried out (details of the heating process is described in the Experimental part).

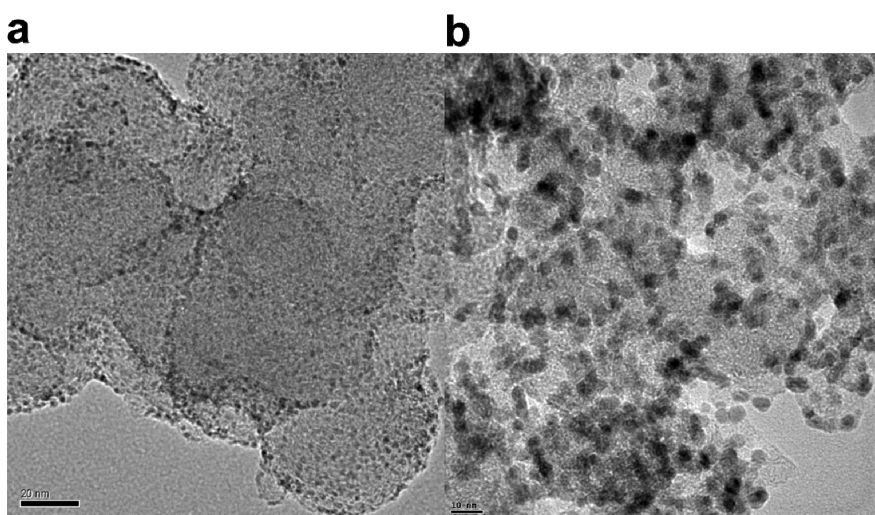


**Figure S2.** TEM images of as-prepared (a) Ru/C (21.1 wt %) and (b) Pd/C (28.4 wt %).

In the case of Pd nanoparticles, which had the average diameter of Pd was ca. 5.5 nm, the peak of Pd(111) was placed in the range of  $2\theta$  from  $38.2^\circ$  to  $38.8^\circ$ . This indicates that the lattice of Pd particles is expanded, as compared to its bulk state. It was very difficult to solve this problem before we found that the expanded structure originated from the carbon contamination in a Pd lattice, as described in reference no. 32. By heating the PdCx in Air atmosphere, we removed dissolved carbon impurities in the Pd lattice, and then, reduced surface oxide by heating them in the flow of the mixture gas of 5 vol.% of H<sub>2</sub> and Ar.

### 3. TEM images and particle size distribution histograms of Pd/C, Pt[0.1]/Pd/C, Pt[0.3]/Pd/C, and Pt[0.5]/Pd/C

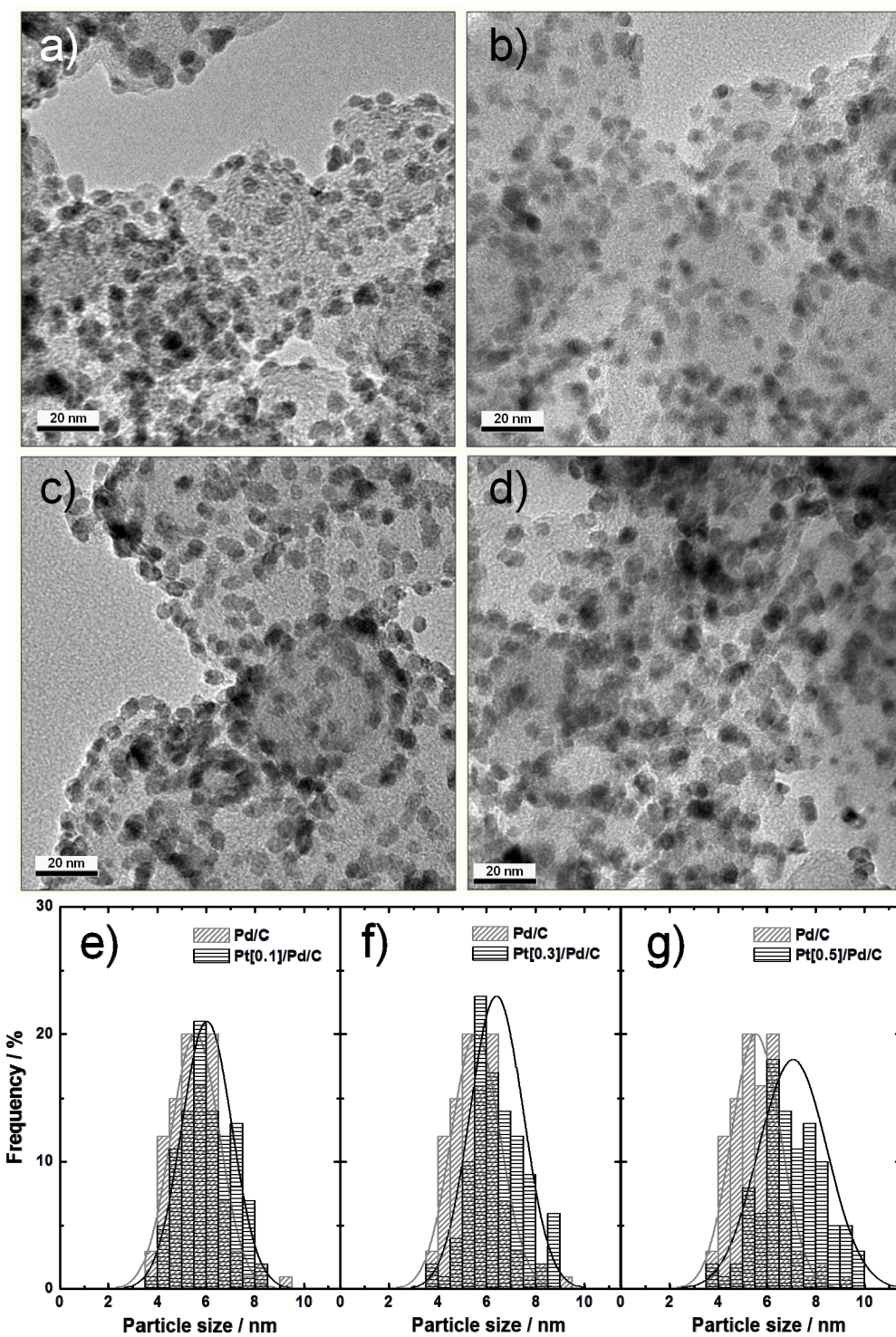


**Figure S3.** TEM images of (a) Pd/C, (b) Pt[0.1]/Pd/C, (c) Pt[0.3]/Pd/C, and (d) Pt[0.5]/Pd/C. Particle size distribution histograms of (e) Pt[0.1]/Pd/C, (f) Pt[0.3]/Pd/C, and (g) Pt[0.5]/Pd/C obtained from (b), (c), and (d), respectively.

We present the additional TEM images of Pt/Pd/C with various loading amounts of Pt, as shown in Fig. S3. The loading amount of Pd (28.4 wt %) corresponds to 40 wt % of Pt because molar volume and weight of Pt are larger than them of Pd. 40 wt % loading of nano-sized Pt is relatively high, considering the surface area of carbon black (ca. 250 m<sup>2</sup>/g). As observed in TEM images of the heat-treated Pd/C of Fig. S3a, Pd nanoparticles are densely distributed on the carbon surface. As the amount of Pt in the surface layer increases, the gradual increase in particle size becomes more apparent, as shown in the size distribution histograms of Figure S3e,f, and g, although the increase of Pt loading causes the decrease in the mass-specific active surface area due to the connection between particles.

#### 4. ORR currents of Pt[0.2-1.4]/Ru/C and Pt[0.1-0.7]/Pd/C

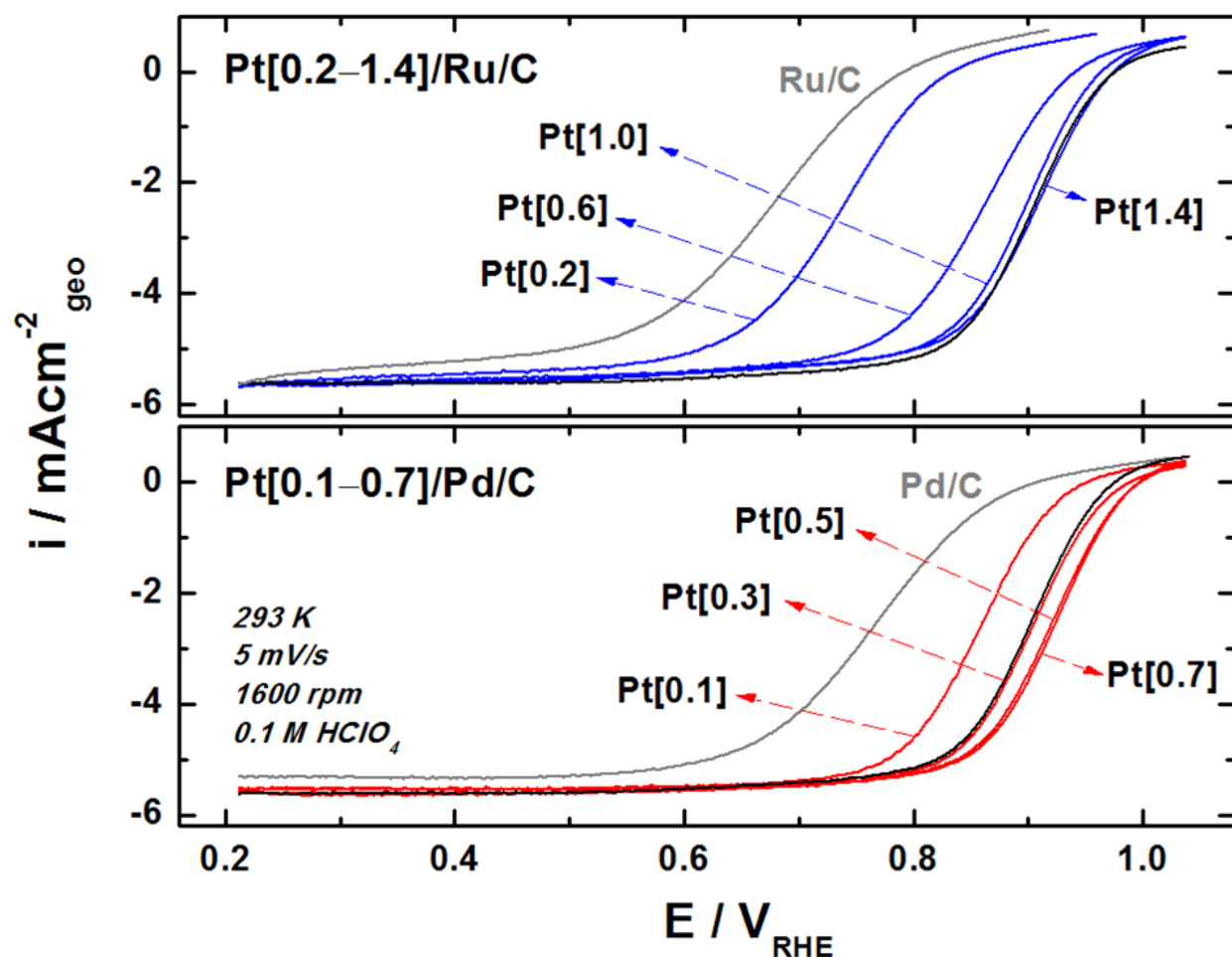


**Figure S4.** Comparison of the ORR polarization curves for 40 wt % Pt/C (JM) (black line), Ru-Pt[0.2–1.4] (upper part) and Pd-Pt[0.1–0.7] (lower part) core–shell nanoparticles supported on carbon black.

It is note-worthy that Pt[0.3]/Pd/C has the slightly higher activity (0.900 V vs RHE of a half-wave potential) than that of commercial Pt/C (40 wt %, JM) (0.897 V vs RHE).

## 5. Refined lattice parameters of Ru-Pt core-shell nanoparticles from powder X-ray diffraction

Table S1 shows the refined lattice parameters of Ru-Pt core-shell nanoparticles, which were obtained from synchrotron powder X-ray diffraction (PXRD). Figure 3b was plotted from this table.

**Table S1.** Refined lattice parameter of Ru-Pt core-shell nanoparticles.

bulk Pt <sup>a</sup>	refined lattice parameters (Å)			
	Pt[0.6]/Ru/C	Pt[1.0]/Ru/C	Pt[1.4]/Ru/C	Pt[1.6]/Ru/C
3.9230	3.8376	3.8613	3.8801	3.9033

<sup>a</sup> the lattice parameter of bulk Pt is calculated from JCPDS of Pt (no. 004-0802).

## 6. Detailed EXAFS parameters of Pd- and Ru-Pt core-shell nanoparticles

Table S2 and S3 show EXAFS parameters extracted from  $k^3$ -weighted Pt L<sub>III</sub> spectra of Pt/C and Pd-Pt and Ru-Pt core-shell particles supported on carbon black.

**Table S2.** Results of model fitting of  $k^3$ -weighted and Fourier-filtered Pt L<sub>III</sub> EXAFS for Pd-Pt.

Sample	Bond	N	R (Å)	$\sigma^2$ (Å <sup>2</sup> )	$\Delta E$ (eV)	$R_{factor}$ (%)
Pt/C (JM)	Pt-O	1.4 (3)	2.00 (1)	0.0033		
	Pt-Pd	N/A	N/A	N/A	6.3 (8)	0.5
	Pt-Pt	6.6 (5)	2.76 (1)	0.0066 (4)		
Pt[0.1]/Pd/C	Pt-O	0.9 (1)	1.97 (1)	0.0033*		
	Pt-Pd	2.2 (4)	2.70 (1)	0.0068 (17)	2.2 (11)	0.9
	Pt-Pt	3.0 (5)	2.68 (1)	0.0068 (17)		
Pt[0.3]/Pd/C	Pt-O	1.0 (1)	1.98 (1)	0.0033*		
	Pt-Pd	1.8 (2)	2.72 (1)	0.0075 (15)	2.6 (9)	0.4
	Pt-Pt	4.8 (7)	2.70 (1)	0.0075 (15)		
Pt[0.5]/Pd/C	Pt-O	0.8 (1)	2.00 (1)	0.0033*		
	Pt-Pd	1.7 (2)	2.74 (1)	0.0079 (9)	4.2 (9)	0.5
	Pt-Pt	6.0 (7)	2.73 (1)	0.0079 (9)		
Pt[0.7]/Pd/C	Pt-O	0.6 (1)	1.99 (1)	0.0033*		
	Pt-Pd	1.4 (1)	2.72 (1)	0.0079 (7)	4.3 (8)	0.4
	Pt-Pt	6.8 (7)	2.72 (1)	0.0079 (7)		
Pt[0.9]/Pd/C	Pt-O	1.1 (1)	2.00 (1)	0.0033*		
	Pt-Pd	1.1 (1)	2.73 (1)	0.0072 (6)	5.0 (8)	0.2
	Pt-Pt	6.4 (6)	2.74 (1)	0.72 (6)		

1. Notation: N, coordination number; R, interatomic distance;  $\sigma^2$ , Debye-Waller factor;  $\Delta E$ , energy-shift;  $R_{factor}$ , goodness of fit which gives a sum-of-squares measure of the fractional misfit.

2. \*fixed parameter.

3. The value in parenthesis denotes the estimated error of the calculated parameter.

**Table S3.** Results of model fitting of  $k^3$ -weighted and Fourier-filtered Pt L<sub>III</sub> EXAFS for Ru-Pt.

Sample	Bond	N	R (Å)	$\sigma^2$ (Å <sup>2</sup> )	$\Delta E$ (eV)	$R_{factor}$ (%)
Pt/C (JM)	Pt-O	1.4 (3)	2.00 (1)	0.0033		
	Pt-Ru	N/A	N/A	N/A	6.3 (8)	0.005
	Pt-Pt	6.6 (5)	2.76 (1)	0.0066 (4)		
Pt[0.2]/Ru/C	Pt-O	0.7 (4)	2.04 (4)	0.0033*		
	Pt-Ru	1.6 (5)	2.67 (2)	0.0062 (28)	2.1 (26)	0.041
	Pt-Pt	4.0 (7)	2.68 (2)	0.0062 (28)		
Pt[0.6]/Ru/C	Pt-O	1.1 (2)	1.99 (1)	0.0033*		
	Pt-Ru	1.6 (3)	2.70 (1)	0.0056 (19)	4.4 (18)	0.018
	Pt-Pt	3.4 (9)	2.71 (1)	0.0056 (19)		
Pt[1.0]/Ru/C	Pt-O	1.1 (1)	2.00 (1)	0.0033*		
	Pt-Ru	0.9 (2)	2.70 (3)	0.0089 (14)	3.7 (19)	0.006
	Pt-Pt	0.9 (2)	2.70 (3)	0.0089 (14)		
Pt[1.4]/Ru/C	Pt-O	0.8 (1)	1.99 (1)	0.0033*		
	Pt-Ru	1.0 (1)	2.71 (1)	0.0082 (7)	4.4 (9)	0.004
	Pt-Pt	6.3 (7)	2.72 (1)	0.0082 (7)		
Pt[1.6]/Ru/C	Pt-O	0.6 (1)	2.01 (2)	0.0033*		
	Pt-Ru	0.6 (1)	2.72 (2)	0.0070 (7)	4.5 (10)	0.003
	Pt-Pt	6.8 (8)	2.73 (1)	0.70 (7)		

1. Notation: N, coordination number; R, interatomic distance;  $\sigma^2$ , Debye-Waller factor;  $\Delta E$ , energy-shift;  $R_{factor}$ , goodness of fit which gives a sum-of-squares measure of the fractional misfit.

2. \*fixed parameter.

3. The value in parenthesis denotes the estimated error of the calculated parameter.